

## Accepted Manuscript

Title: Kinetics and mechanism of Paraquat's degradation:  
UV-C photolysis vs UV-C photocatalysis with TiO<sub>2</sub>/SiC foams

Authors: Cédric B.D. Marien, Marie Le Pivert, Antonin Azaïs,  
Ignace Christian M'Bra, Patrick Drogui, Ahmad Dirany,  
Didier Robert



PII: S0304-3894(18)30449-7  
DOI: <https://doi.org/10.1016/j.jhazmat.2018.06.009>  
Reference: HAZMAT 19446

To appear in: *Journal of Hazardous Materials*

Received date: 14-12-2017  
Revised date: 28-5-2018  
Accepted date: 3-6-2018

Please cite this article as: Marien CBD, Le Pivert M, Azaïs A, M'Bra IC, Drogui P, Dirany A, Robert D, Kinetics and mechanism of Paraquat's degradation: UV-C photolysis vs UV-C photocatalysis with TiO<sub>2</sub>/SiC foams, *Journal of Hazardous Materials* (2018), <https://doi.org/10.1016/j.jhazmat.2018.06.009>

This is a PDF file of an unedited manuscript that has been accepted for publication. As a service to our customers we are providing this early version of the manuscript. The manuscript will undergo copyediting, typesetting, and review of the resulting proof before it is published in its final form. Please note that during the production process errors may be discovered which could affect the content, and all legal disclaimers that apply to the journal pertain.

## **Kinetics and mechanism of Paraquat's degradation: UV-C photolysis vs UV-C photocatalysis with TiO<sub>2</sub>/SiC foams**

Cédric B. D. Marien<sup>1,2</sup>, Marie Le Pivert<sup>1</sup>, Antonin Azaïs<sup>1</sup>, Ignace Christian M'Bra<sup>2</sup>, Patrick Drogui<sup>1</sup>, Ahmad Dirany<sup>1</sup> and Didier Robert<sup>2\*</sup>

<sup>1</sup>Institut national de la recherche scientifique (INRS - Eau, Terre et Environnement), Université du Québec, 490 rue de la Couronne, Québec city, Québec, Canada G1K 9A9

<sup>2</sup>Institut de Chimie et Procédés pour l'Energie, l'Environnement et la Santé (ICPEES), CNRS-UMR7515-University of Strasbourg, Saint-Avold Antenna, Université de Lorraine, 12 rue Victor Demange, 57500 Saint-Avold, France.

\*Corresponding author: [Didier.robert@univ-lorraine.fr](mailto:Didier.robert@univ-lorraine.fr)

### **Highlights**

- Complete mineralization of Paraquat herbicide par PCO
- Proposition of mechanism for Paraquat's degradation by photocatalysis or photolysis under UV-C radiation
- Use of 3D photocatalytic materials for water treatment

**Abstract**

In this study, the photolytic and photocatalytic removal of the herbicide paraquat is investigated under UV-C (254 nm). For photocatalytic experiments, SiC foams were used with P25-TiO<sub>2</sub> nanoparticles deposited by dip-coating. The foams were characterized by scanning electron microscopy and paraquat's degradation under UV-C photolysis or photocatalysis, followed by UV-vis spectroscopy, total organic carbon analyzer, LC-MS and ion chromatography. After 3 hours of reactions by photolysis and photocatalysis, 4% and 91% of TOC removal were observed. An analysis of degradation by-products showed a similar degradation pathway with pyridinium ions observed by LC/MS and carboxylic acids (succinate, acetate, oxalate and formate) detected by ion chromatography. In conclusion, these two different photo-degradation processes are able to remove paraquat and produce similar by-products. However, the kinetics of degradation is rather slow during photolysis and it is recommended to combine the UV-C lightning with a TiO<sub>2</sub> photocatalyst to improve the mineralization rate.

**Keywords:** advanced oxidation process, photocatalysis, photolysis, TiO<sub>2</sub>, SiC foam

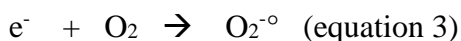
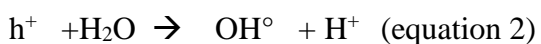
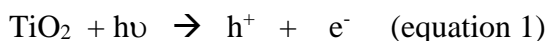
## 1 Introduction

Pollution is a worldwide problematic concerning water, air or soil quality. Now, it is observed in many countries that intensive agriculture causes troubles related to the use of harmful pesticides and/or herbicides contaminating surface waters (rainwater runoff), soils (crops) and air (spray application). In this study, the attention is focused on Paraquat (or Gramoxone), an herbicide used in more than 130 countries over the last decades [1]. This compound is mainly used for crops preparation by spray application. Unfortunately, its use is correlated to Parkinson's disease for farmers or residents living close to those crops and exposed during spray application [2,3]. Some precautions should thus be taken in order to avoid the use of such compound.

Paraquat is also applied for aquatic weed control from 0.5 to 1.5 ppm [4] and unfortunately, it was shown that concentrations as low as 0.1 ppm resulted in abnormal tail flexure on *Xenopus Laevis* [5]. Consequently, recommendation guidelines suggest Paraquat concentration lower than 0.1 ppb in Europe or 10 ppb in Canada [6].

The search for new treatment methods able to degrade such recalcitrant compound is under way. Currently, advanced oxidation processes (AOPs) are very attractive thanks to the production of highly oxidizing hydroxyl radicals. Among these processes, photocatalysis is particularly suitable because it does not require the handling of expensive chemicals such as  $H_2O_2$  and hence, it can be operated autonomously. The principle of photocatalysis is based on the use of a photocatalyst (semiconductor), usually  $TiO_2$ , activated by UV-light to produce electron-hole pairs (equations 1), reacting with water (holes-equation 2) and dissolved dioxygen (electrons-equation 3) to produce

respectively the hydroxyl radical  $\text{OH}^\bullet$  and the superoxide radical  $\text{O}_2^{\bullet-}$ .



Over the last decades, many photocatalysts were studied and titanium dioxide is now a reference material due to its high efficiency, its high photochemical stability and its low cost [7-12].

Historically, photocatalysis was operated with  $\text{TiO}_2$  nanoparticles in suspension but the recovery of the photocatalyst was highly challenging. In order to solve this, supported photocatalysis and photocatalytic membrane reactors (PMR) were developed [13]. Unfortunately, the use of PMRs is rather expensive compared to supported photocatalysis because of the complex/energy consuming ultrafiltration membrane system. The advances in the field of supported photocatalysis come from the development of various supports [14] such as glass [15-17]), stainless steel [18,19], silicon carbide [20] or alumina [16].

In order to improve the poor exchange surface of the supported photocatalyst and the effluent in comparison with the  $\text{TiO}_2$  nano-slurries, it is recommended to use three-dimensional supports such as beads [21,22,16], tubes [23,24] or foams [25-27].

Among 3D-support materials, silicon carbide foams are highly suitable due to their high chemical resistance, outstanding thermal stability and their macro-porosity providing a high internal surface enabling the immobilization of large amounts of photocatalyst, usually by dip-coating [26]. The development of such technology is still very recent and

much progress is required especially for the development of photocatalytic reactors integrating TiO<sub>2</sub>/SiC foams.

The photolytic/photocatalytic degradation of paraquat was previously investigated by many groups [28-31]. However in these last works, photolysis and photocatalysis are not compared regarding oxidation by-products, especially under UV-C light sources (UV-C are the rays with a wavelength between 100 and 280 nm). The objectives of our work, is to show that UV-C lights can play a significant role in paraquat's removal. On the other hand, we have attempted to determine the paraquat degradation mechanism by measuring the Total Organic Carbon (TOC) during irradiation as well as the concentration of paraquat and its degradation by-products by UV-Visible spectroscopy and LC-MS (Liquid chromatography–mass spectrometry).

## 2 Experimental section

### *Reactants and chemicals*

Paraquat dichloride hydrate (98%), anhydrous ethanol and acetone were provided from Sigma Aldrich. TiO<sub>2</sub> nanoparticles (Aeroxide P25) were provided from Evonik. TiO<sub>2</sub> P25 is a fine white powder with hydrophilic character caused by hydroxyl groups on the surface. It consists of aggregated primary particles. The aggregates are several hundred nm in size and the primary particles have a mean diameter of approx. 21 nm. Particle size and density of ca. 4 g/cm<sup>3</sup> lead to a specific surface of approx. 50 m<sup>2</sup>/g. The weight ratio of anatase and rutile is approximately 80 / 20.

### *Preparation of SiC foams*

SiC foams were kindly provided by the SICAT company (Germany) and their synthesis is described in detail elsewhere [32]. These foams were shaped as cylinders (diameter = 35 mm, length = 50 mm) and each foam weighs approximately 10 g (figure 1). Before dip coating, the foams were ultrasonicated in acetone, ethanol and water. Finally they were dried at 110°C overnight in an electric oven.

### *Deposition of P25 on SiC foams by dip-coating*

Immobilization of TiO<sub>2</sub>-P25 photocatalyst was performed by preparing a slurry (100 g/l of P25 in anhydrous ethanol, Aldrich) under ultrasonication for 30 minutes. The reasons that explain the high efficiency of TiO<sub>2</sub>-P25 are not yet fully known. It is likely that the main reasons are the high hydroxylation of its surface combined with a lower recombination rate of electron/hole pair. There is also the creation of a heterojunction between anatase and rutile phases. SiC foams were then immersed in the suspension at 8 mm/s and five dipping cycles were performed for each foam (approximately 10 g without TiO<sub>2</sub>) with 10 min drying between consecutive immersions. After that, each foam was dried overnight at 110°C and heated for 4 hours at 450°C with a heating ramp of 5°C/min under air in a Nabertherm oven. For each foam, 16 ± 1 wt% of TiO<sub>2</sub> was immobilized.

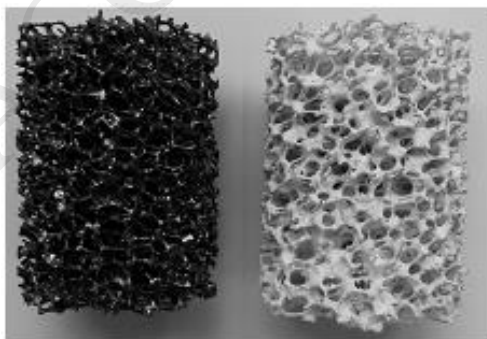


**Figure 1:** SiC foam uncoated (black) and coated by TiO<sub>2</sub> P25 (white).

### SEM analysis

SiC foams coated by TiO<sub>2</sub> P25 were characterized by scanning electron microscopy at 20 kV with a Zeiss apparatus model EVO 50 equipped with a tungsten filament cathode. For analysis, a small fragment of a TiO<sub>2</sub>/SiC foam was inserted in the SEM with a carbon adhesive tape from Soquelec.

### Photocatalytic reactor

The photocatalytic reactor is presented in detail on figure 2.

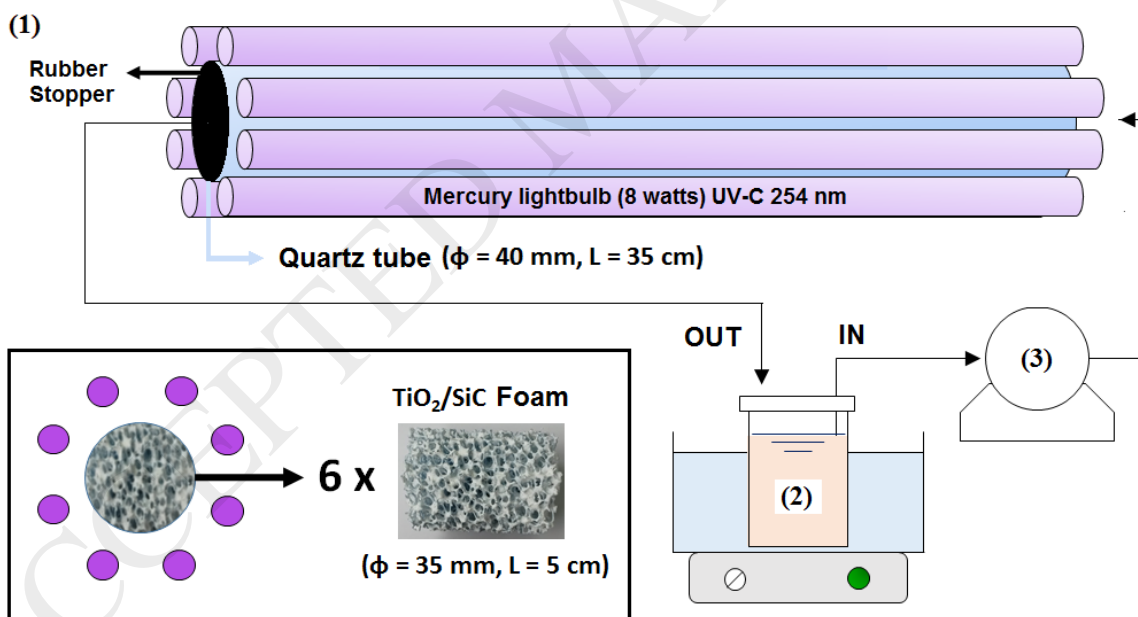


**Figure 2:** Photocatalytic tubular reactor made with (1) a UV-C lightning system + a quartz tube + 6 TiO<sub>2</sub>/SiC foams, (2) a paraquat solution and (3) a peristaltic pump.

Six TiO<sub>2</sub>/SiC foams were inserted in the reactor in a quartz tube (diameter 40 mm; length



30 mm) separated from 6 UV-C lamps (1 cm between the quartz tube and the lamps). Effluent inlet and outlet diameters are 5 mm. Each lamp is an 8 watts Mercury bulb with a maximum emission wavelength at 254 nm (G8T5 from Hitachi). The reactor was connected to a peristaltic pump (Masterflex L/S, Cole Parmer) to control the flow rate of the solution into the photoreactor. Prior to each experiment, photo-reactor was cleaned with water for one hour of irradiation with TiO<sub>2</sub>/SiC foams in order to obtain reproducible experiments (twice for each experiment). For each experiment, the treated volume was 1 liter and the reactor was operated under recirculation. The lamps were left 10 minutes heating until the light intensity was stable and then the feed solution of paraquat was pumped inside the tube at  $t = 0$  min.

#### *Probe molecule and UV-vis spectroscopy*

To evaluate the photocatalytic performances of the reactor, Paraquat was used as a probe molecule. The concentration (5 to 40 ppm) of this compound was followed by UV-vis spectroscopy at 257 nm (maximum absorption wavelength) with a UV-Visible apparatus (Agilent Cary 50).

#### *Total Organic Carbon (TOC) analysis*

Total organic carbon measurements were determined by the non-purgeable organic carbon method, on a Shimadzu VCPH apparatus with a very low sensitivity (detection limit = 0.05 mg Carbon per liter).

#### *LC-MS analysis*

By-products of degradation were identified by LC-MS with a TSQ Quantum Access apparatus from Thermo Scientific. Sample injection was performed for 6 minutes with 20  $\mu$ l/min mixed with the eluant and injected at 0,2 ml/min with an eluant composed of 87.5 % of solution A (water + 30 mM of ammonium formate + 0.1 % of formic acid) and 12.5 % of solution B (acetonitrile + 30 mM of ammonium formate + 0.1% formic acid). The analyte and eluant were then injected in a chromatographic column: Hypersil Gold from Thermo Scientific (100mm x 2,1 mm) heated at 35°C.

#### *Ion chromatography*

Organic acids were detected by ion chromatography with an ionic resin (Ion PAC AS11-HC at 30°C) set on an Integrion HPIC apparatus from Thermo. Elution was programmed with a concentration gradient of KOH between 1 and 30 mM. A cationic suppressor is then used to remove cations and then a conductivity detector was used for concentration determination at 35°C. Detection limits were in the range 0.001 to 0.002 mg/l for each compound.

## **Results and discussion**

### ***A. Characterization of TiO<sub>2</sub> coated SiC foams***

The dip-coating technique allows to obtain highly homogeneous and evenly coated TiO<sub>2</sub>/SiC foams. A picture of a foam before and after dip/coating in the TiO<sub>2</sub> suspension is presented as additional information (figure 1). After annealing at 450°C, the coated

foam was characterized by scanning electron microscopy (figure 3). Macro-pores were observed in the range 3 to 5 mm. The coating is quite homogeneous but the presence of cracks is highlighted at the microscale due to the strains during the drying step (dip-coating) or the annealing step at 450°C. This suggests that the deposition method must be improved for future works.

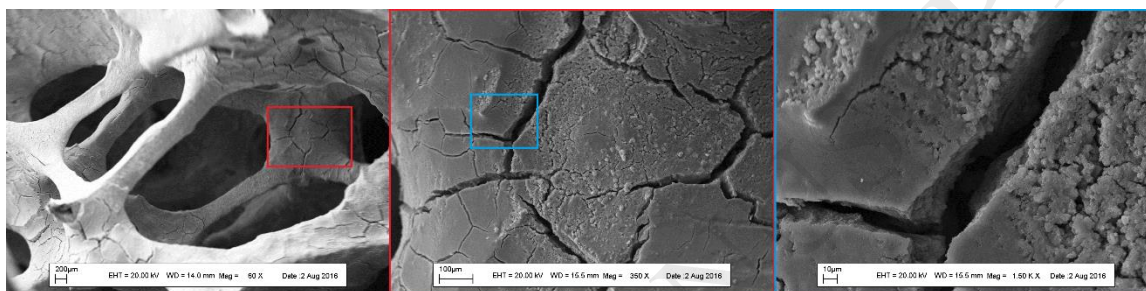


**Figure 3:** SEM characterization of SiC foams coated by Aeroxide P25. Scale-bar : 200 μm (left), 100 μm (middle), 10 μm (right).

## ***B. Comparison between photolysis, photocatalysis and adsorption in the dark***

### ***a. Degradation followed by UV-visible spectroscopy***

The comparison between the three main processes involved (adsorption in the dark, UV-C photolysis and UV-C photocatalysis) is presented in figure 4. The photolysis experiment was performed without TiO<sub>2</sub>/SiC foams inside the reactor. It is found that UV-C photolysis and pollutant adsorption have a small effect on Paraquat removal. The removal of paraquat using the adsorption process (in the dark) was 30% after 3 h of treatment, whereas 50% of paraquat was removed using direct UV-C photolysis process. By comparison, when UV-C irradiations were combined with a TiO<sub>2</sub>-supported

photocatalyst, 100% of Paraquat was removed after the same treatment time.

This ability to remove paraquat faster with a photocatalytic treatment is due to the production of the hydroxyl radical, a strong oxidizing agent. Indeed, under UV irradiation, electrons ( $e^-$ ) of the  $\text{TiO}_2$  semi-conductor are excited from the valence band (VB) to the conduction band (CB), thereby creating holes ( $h^+$ ) in the valence band. These charge carriers ( $e^-/h^+$ ) are then separated and react at the surface of the photocatalyst, where they are then available to undergo redox reactions with pollutants thanks to the production of oxidizing species: production of superoxide radicals on the conduction band via reduction of dissolved oxygen or dissociation of water by holes to create the hydroxyl radical.

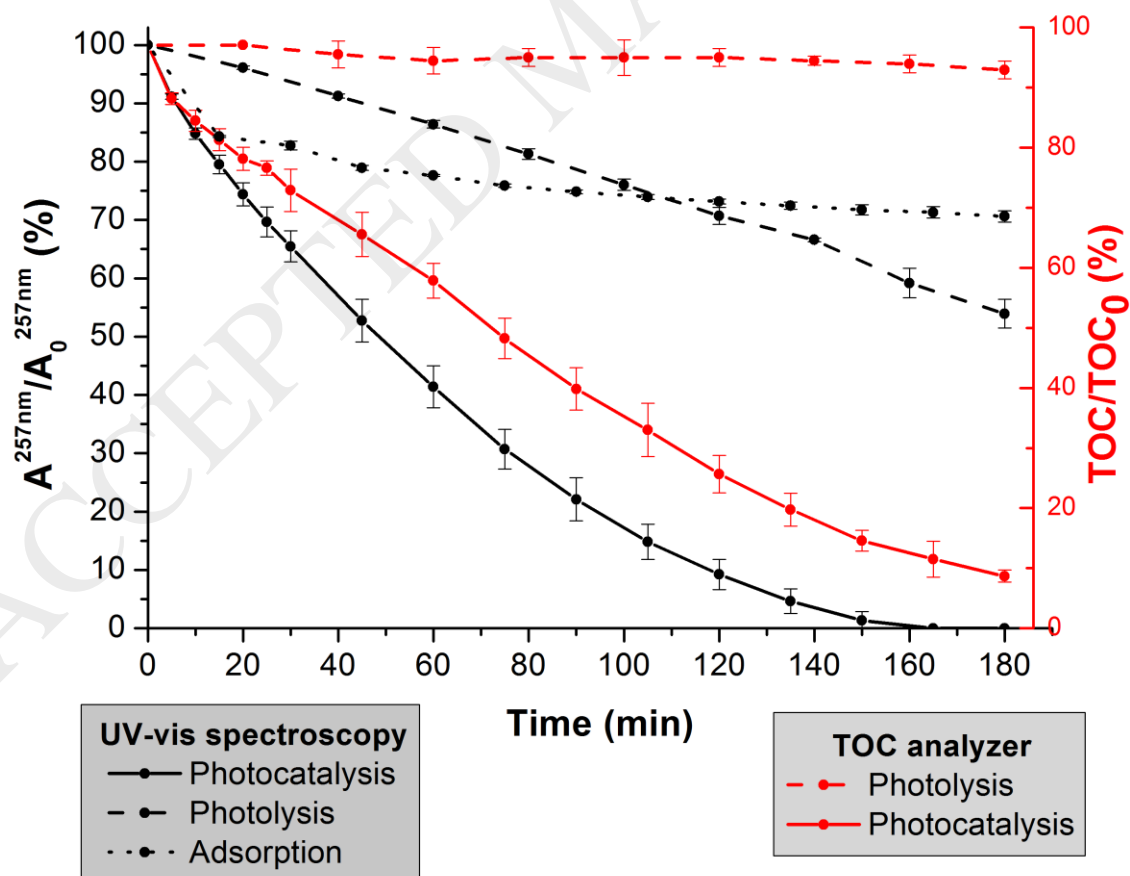


**Figure 4:** Comparison between adsorption, photolysis and photocatalysis at 5 ml/s for an initial [Paraquat] = 20 ppm with 6 UV-C lamps. Processes were followed by UV-vis spectroscopy at 257 nm ( $\lambda_{\max}$  of Paraquat) or by total organic carbon analyzer (TOC). Each experiment is performed twice. For photolysis experiments, TiO<sub>2</sub>/SiC foams were not in the photo-reactor.

There is a direct relationship between paraquat absorbance of UV radiation and its degradation by photolysis under UVC. Due to the overlapping between the emission spectra of the UV-C lamp (254 nm) and the absorption spectra of Paraquat (max. absorption wavelength = 257 nm), electronic transitions must occur in Paraquat molecules. However, it is difficult to establish a consistent ratio because paraquat removal by UVC irradiation is much faster than for other wavelengths (unpublished results). In addition, the paraquat degradation by-products play a role in the degradation processes for example, via screening the UV radiation. Paraquat has high molar absorptivity in the UV region. On the other hand, in direct photolysis of paraquat at 254 nm, low concentrations of H<sub>2</sub>O<sub>2</sub> are formed. The photolysis of the hydrogen peroxide does not compete with paraquat because the primary quantum yield of H<sub>2</sub>O<sub>2</sub> at 254 nm is very high. It is thought that H<sub>2</sub>O<sub>2</sub> formed could undergo some photolysis. If this is the case, hydroxyl radicals would form and oxidation of atrazine would be due to both direct photolysis and OH° radical reactions. These two reasons explain the decrease in Paraquat concentration during photolysis.

***b. Degradation followed by TOC analyzer***

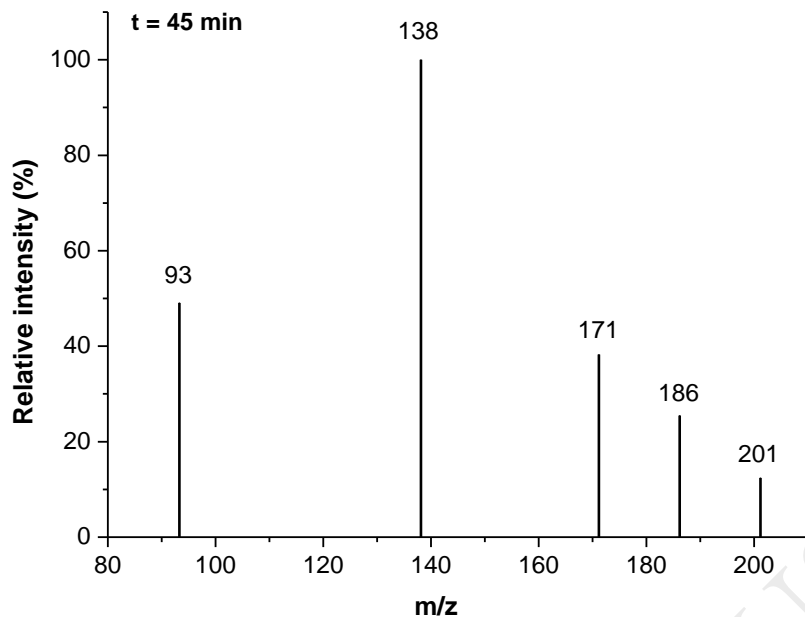
In order to compare the efficiency of photolysis and photocatalysis towards mineralization, organic matter (paraquat + by-products) was followed by TOC analysis. Results are presented in figure 4. Photolysis is able to degrade paraquat selectively, but

TOC analysis reveals that less than 5% TOC is mineralized after 180 minutes of UV-C photolysis. On the other hand, photocatalysis is very efficient because 90 % of organic matter is removed after 180 minutes due to the ability of this process to produce the hydroxyl radicals allowing paraquat and its by-products to be converted to CO<sub>2</sub>, inorganic salts and water.

***C. By-products formation and proposed mechanism of paraquat degradation***

***a. Evolution of pyridinium compounds***

In order to understand which compounds were mineralized by photocatalysis, paraquat by-products were analyzed by LC-MS and ion chromatography. First, LC-MS allowed to follow known by-products of degradation, based on a literature review, especially pyridinium compounds. The mass spectra obtained after 45 minutes of degradation by photocatalysis are presented in figure 5. Unknown by-products of degradation were not observed during experiments in the time range studied (0-120 min).

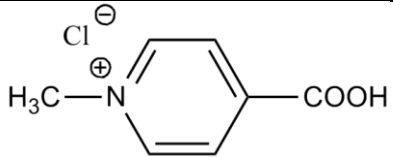
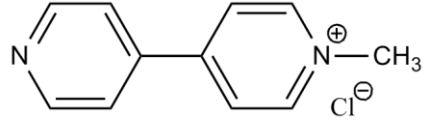
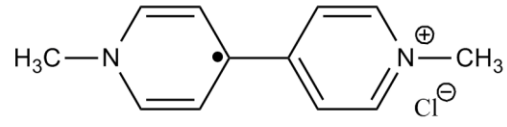
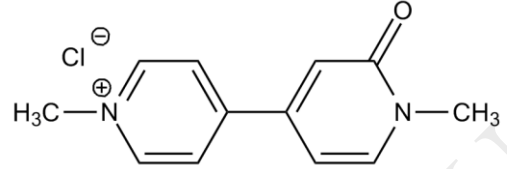


**Figure 5:** Mass spectra obtained after 45 minutes of photocatalytic degradation with an initial paraquat concentration of 10 ppm.

Many m/z peaks were observed: 93, 138, 171, 186 and 201. These species were previously identified and attributed to the compounds listed in table 1.

**Table 1:** Chemical structure of identified m/z ratios based on literature review.

Nom	Structure	m/z	Source
Paraquat		93	[28-33]

<b>4-carboxy-1-methyl pyridinium ion</b>		138	[28,34,35]
<b>Monoquat</b>		171	[28,34,35]
<b>Reduced Paraquat</b>		186	[28,33,36]
<b>Paraquat monopyrindone</b>		201	[28,34,35]

Paraquat has an atomic mass of 186 with  $z = 2$  and hence, an  $m/z$  ratio appears at  $= 93$ . Besides, the peak at  $m/z = 186$  also appears because the reduced form of paraquat molecules is stabilized by resonance [28].

Another compound, monoquat, appears at  $m/z = 171$  and corresponds to paraquat with a loss of  $-CH_3$  on the pyridinium group ( $m/z = 186 - 15$ ). Another structure can be observed at  $m/z = 201$  and was previously attributed to paraquat monopyrindone [28, 34-35]. Besides, during the degradation, an intense peak appears at  $m/z = 138$  on the mass spectra and corresponds to a by-product: 4-carboxy-1-methyl pyridinium ion [28, 34-35].

The kinetics of appearance/degradation of each  $m/z$  compound is shown in figure 6 with relative peak intensities as a function of the time of degradation. Experiments reveal that initial paraquat solution contains a mix of paraquat ( $m/z = 93$ ), reduced paraquat ( $m/z = 186$ ), monoquat ( $m/z = 171$ ) and Paraquat monopyrindone ( $m/z = 201$ ). The only compound that is produced during the degradation and observed by LC-MS has an  $m/z$



ratio equal to 138. Besides, it appears that only photocatalysis is able to degrade this compound ( $m/z = 138$ ) while photolysis only leads to its accumulation in the solution.

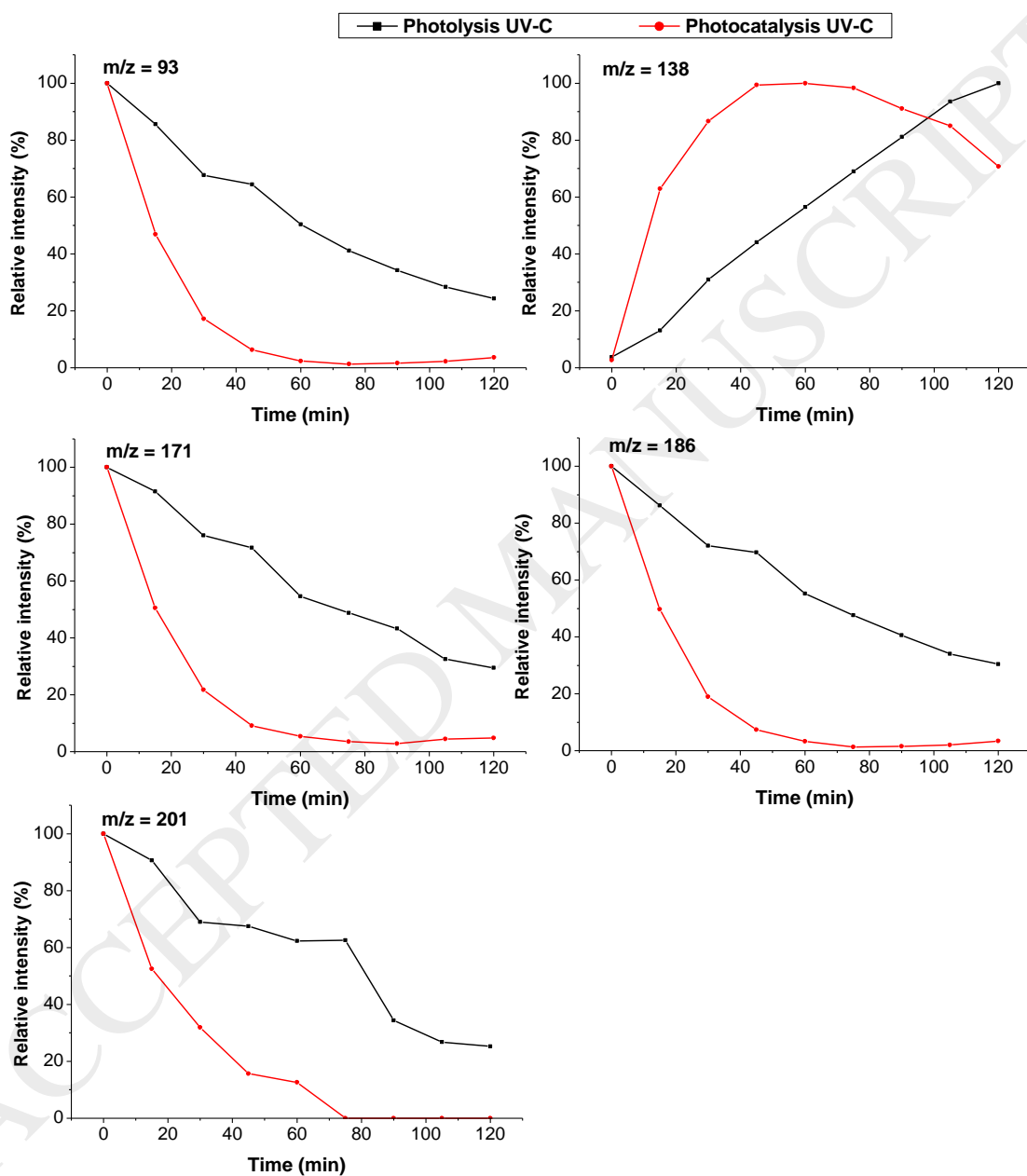


**Figure 6:** Kinetics of degradation for various  $m/z$  compounds in solution by LC-MS observed by photolysis or photocatalysis at 5 ml/s for an initial [Paraquat] = 10 ppm with 6 UV-C lamps. Each experiment was performed twice.

*b. Evolution of short-chain carboxylic acids*

Other by-products were detected by ion chromatography, especially short-chain organic acids. These compounds were detected as carboxylated anions at different elution time: 8.9 min (acetate), 10.5 min (formate), 19.6 min (succinate), 20.4 min (maleate) and 21.6 min (oxalate). Concentration profile for each carboxylate compound is shown in figure 7. These by-products accumulate in the solution during photolytic treatment. Besides, the photocatalytic treatment allows their degradation due to the production of the hydroxyl radical. Interestingly, maleate was only observed during photolytic treatments. On the other hand, succinate appears to be the most concentrated by-product during the photocatalytic degradation of paraquat.

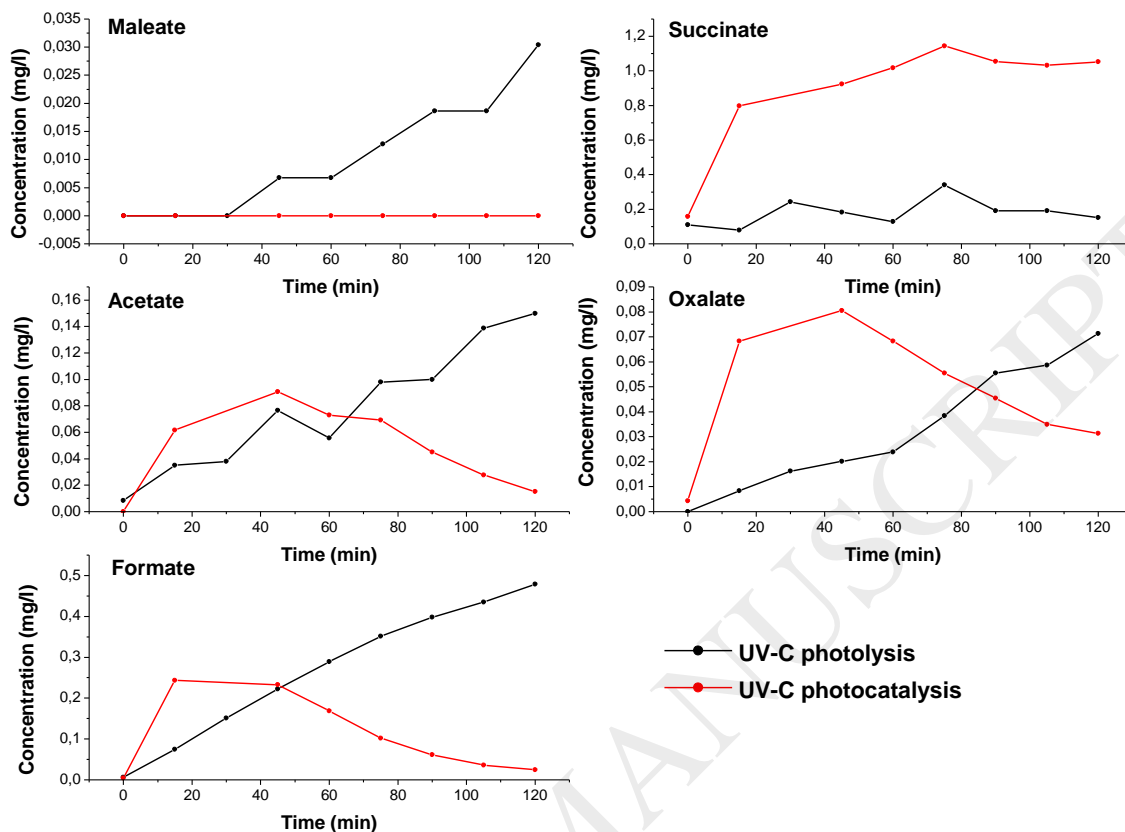


**Figure 7:** Kinetics of degradation/appearance of various organic acids produced by photocatalysis and photolysis and detected by ion chromatography. The experiments were performed in the photo-reactor at 5 ml/s for an initial [Paraquat] = 10 ppm with 6 UV-C lamps. Each experiment was performed twice.

### *c. Proposed degradation pathway*

Thanks to LC-MS and ion chromatography, a paraquat mechanism of degradation is proposed as shown in figure 8. Paraquat molecules are first converted to similar molecular structures bearing bipyridinium group (monoquat, reduced paraquat or paraquat monopyridone). Then fragmentation occurs and leads to lower molecular weight compounds. 4-carboxy-1-methylpyridinium ion and short chain carboxylic acids appears to be the major by-products. Mineralization experiments suggest that only photocatalysis

is able to degrade these species to the ultimate products of oxidation, especially CO<sub>2</sub>.

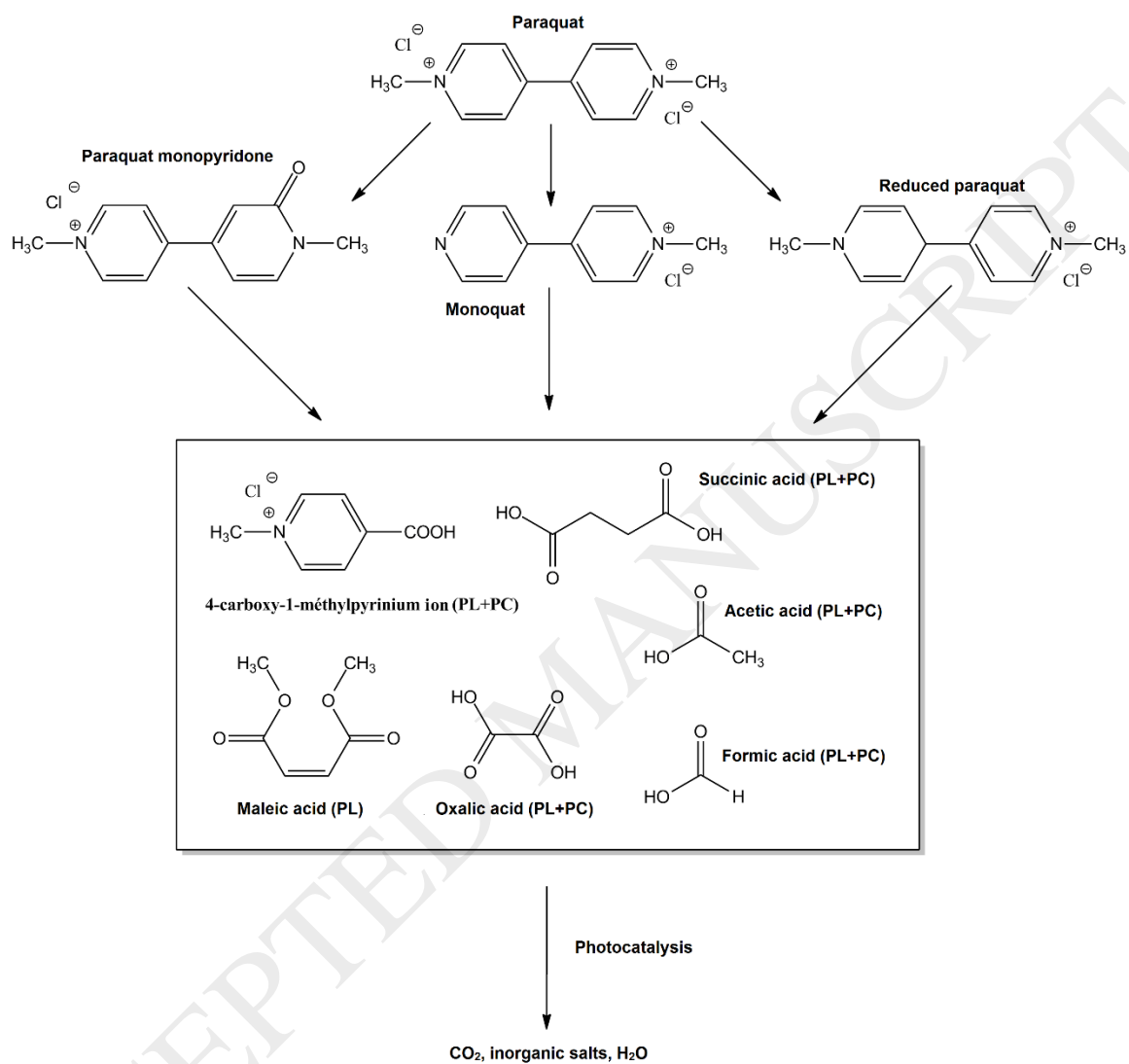


**Figure 8:** Proposed mechanism for Paraquat degradation by photocatalysis or photolysis under UV-C radiation.

### 3 Conclusion

This paper presents a critical comparison between UV-C photolysis and UV-C

photocatalysis for the degradation of paraquat molecules. Experiments reveal that photolysis is able to degrade this compound but cannot lead to its mineralization. Besides, photocatalysis is very effective for removing paraquat and its by-products as shown by mineralization studies. The degradation pathway was evidenced through LC-MS and ion chromatography analysis. It appears that similar by-products (pyridinium ions or short-chain carboxylic acids) were formed during both types of treatments (photolysis or photocatalysis) apart for maleate that was only produced during photolytic degradation. The elevated degradation efficiency of photocatalysis is attributed to the production of the  $\text{OH}^\bullet$  radical allowing a complete mineralization. Despite the poor efficiency of photolysis, short-chain carboxylic acids were produced and we suggest that a coupling with a biological reactor could be an interesting perspective to remove paraquat.

#### **4 Acknowledgements**

The authors wish to thank the Région Alsace (France) and the INRS (Québec) for the PhD research grant of Cédric Marien, and SiCat Company for the samples of SiC foams.

#### **5 Bibliography**

- [1] T.O Ikpesu, Assessment of occurrence and concentrations of paraquat dichloride in water, sediments and fish from Warri River Basin, Niger Delta, Nigeria. *Environ. Sci. Pollut. Res.* 22(2014)8517–8525
- [2] M.Brouwer, A. Huss, M. van der Mark, P.C.G. Nijssen, W.M. Mulleners, A.M.G. Sas, T. van Laar, G.R. de Snoo, H. Kromhout, R.C.H. Vermeulen, Environmental exposure to pesticides and the risk of Parkinson's disease in the Netherlands. *Environ. Int.* 107(2017) 100–110
- [3] J.G. Smith, Paraquat poisoning by skin absorption: a review. *Hum. Toxicol.* 7(1988) 15–19
- [4] A. Calderbank, Environmental considerations in the development of diquat and

- paraquat as aquatic herbicides (1971)51–54.
- [5] P. Mantecca, S. Panseri, R. Bacchetta, C. Vismara, G. Vailati, M. Camatini,. Histopathological effects induced by paraquat during *Xenopus laevis* primary myogenesis. *Tissue Cell*, 38(2006)209–217
- [6] D.R. Boyd,. *Cleaner, Greener, Healthier: A Prescription for Stronger Canadian Environmental Laws and Policies*. 2015
- [7] J. Chen, F. Qiu, W. Xu, S. Cao, H. Zhu, Recent progress in enhancing photocatalytic efficiency of TiO<sub>2</sub>-based materials. *Appl. Catal. A Gen.* 495(2015) 131–140.
- [8] X. Chen, S.S. Mao,. Titanium dioxide nanomaterials: synthesis, properties, modifications, and applications. *Chem. Rev.* 107(2007)2891–959.
- [9] M.N. Chong, , B. Jin, C.W.K. Chow, C. Saint, Recent developments in photocatalytic water treatment technology: A review, *Water Res.* 44(2010)2997–3027.
- [10] D. Kanakaraju, B.D. Glass, M. Oelgemöller,. Titanium dioxide photocatalysis for pharmaceutical wastewater treatment. *Environ. Chem. Lett.* 12(2014)27–47.
- [11] J. Schneider, M. Matsuoka, M. Takeuchi, J. Zhang, Y. Horiuchi, M. Anpo, D.W. Bahnemann,. *Understanding TiO<sub>2</sub> Photocatalysis: Mechanisms and Materials*. *Chem. Rev.* 114(2014)9919–9986.
- [12] G. Varshney, S.R. Kanel, D.M. Kempisty, V. Varshney, A. Agrawal, E. Sahle-Demessie, R.S. Varma, M.N. Nadagouda, Nanoscale TiO<sub>2</sub> films and their application in remediation of organic pollutants. *Coord. Chem. Rev.* 306(2016)43–64.
- [13] S.I.Patsios, V.C. Sarasidis, A.J. Karabelas, A hybrid photocatalysis-ultrafiltration continuous process for humic acids degradation. *Sep. Purif. Technol.* 104(2013)333–341.
- [14] D. Robert, V. Keller, N.Keller,. *Immobilization of a Semiconductor Photocatalyst on Solid Supports: Methods, Materials, and Applications*, in: Wiley-VCH: Weinheim, G. (Ed.), *Photocatalysis and Water Purification*. 2013 pp. 145–178.
- [15] M.A. Behnajady, N. Modirshahla, N. Daneshvar, M. Rabbani,. Photocatalytic degradation of an azo dye in a tubular continuous-flow photoreactor with immobilized TiO<sub>2</sub> on glass plates. *Chem. Eng. J.* 127(2007)167–176.
- [16] S. Sakthivel, M. Shankar, M. Palanichamy, B. Arabindoo, V. Murugesan,. Photocatalytic decomposition of leather dye Comparative study of TiO<sub>2</sub> supported on alumina and glass beads. *J. Photochem. Photobiol. A Chem.* 148(2002)153–159.
- [17] N. Serpone, E. Borgarello, R. Harris, P. Cahill, M. Borgarello, E. Pelizzetti,. Photocatalysis over TiO<sub>2</sub> supported on a glass substrate. *Sol. Energy Mater.* 14(1986)121–127.
- [18] G. Balasubramanian, D.D.Dionysiou, M.T. Suidan, I. Baudin, J.M. Lâiné,. Evaluating the activities of immobilized TiO<sub>2</sub> powder films for the photocatalytic degradation of organic contaminants in water. *Appl. Catal. B Environ.* 47(2004)73–84.
- [19] J.C. Yu, W. Ho, J. Lin, H. Yip, P.K. Wong,. Photocatalytic Activity, Antibacterial Effect, and Photoinduced Hydrophilicity of TiO<sub>2</sub> Films Coated on a Stainless Steel Substrate. *Environ. Sci. Technol.* 37(2003)2296–2301.
- [20] A.R. Boccaccini, P. Karapappas, J.M. Marijuan, C. Kaya,. TiO<sub>2</sub> coatings on silicon carbide and carbon fibre substrates by electrophoretic deposition. *J. Mater. Sci.* 39(2004)851–859.

- [21] H. Andreas, M. Piotr, Z. Adriana, H. Jan, Photocatalytic activity of TiO<sub>2</sub> immobilized on glass beads, *Physicochemical Probl. Miner. Process.* 45(2010)49-56
- [22] K. Kobayakawa, C. Sato, Y. Sato, A. Fujishima,. Continuous-flow photoreactor packed with titanium dioxide immobilized on large silica gel beads to decompose oxalic acid in excess water. *J. Photochem. Photobiol. A Chem.* 118(1998) 65–69.
- [23] D.K. Lee, I.C. Cho,. Characterization of TiO<sub>2</sub> thin film immobilized on glass tube and its application to PCE photocatalytic destruction. *Microchem. J.* 68(2001)215–223.
- [24] C.M. Ling, A.R. Mohamed, S. Bhatia,. Performance of photocatalytic reactors using immobilized TiO<sub>2</sub> film for the degradation of phenol and methylene blue dye present in water stream. *Chemosphere* 57(2004)547–554.
- [25] H.Hu, W. J. Xiao, J. Yuan, J. W. Shi, M. Chen, X. Shang Guan, W. Feng, Preparations of TiO<sub>2</sub> film coated on foam nickel substrate by sol-gel processes and its photocatalytic activity for degradation of acetaldehyde. *J. Environ. Sci.* 19(2007)80–85.
- [26] N.A. Kouamé, D. Robert, V. Keller, N. Keller, C. Pham, P.Nguyen,. TiO<sub>2</sub>/Beta-SiC foam-structured photoreactor for continuous wastewater treatment. *Environ. Sci. Pollut. Res.* 19(2012)3727–3734.
- [27] J. Yuan, H. Hu, M. Chen, J. Shi, , Shangguan, W.,. Promotion effect of Al<sub>2</sub>O<sub>3</sub>-SiO<sub>2</sub> interlayer and Pt loading on TiO<sub>2</sub>/nickel-foam photocatalyst for degrading gaseous acetaldehyde. *Catal. Today* 139(2008)140–145.
- [28] M.H. Florêncio, E. Pires, A.L. Castro, M.R. Nunes, C. Borges, F.M. Costa,. Photodegradation of Diquat and Paraquat in aqueous solutions by titanium dioxide: Evolution of degradation reactions and characterisation of intermediates. *Chemosphere* 55(2004)345–355.
- [29] E. Leyva, E. Monreal, N. Viuegas, D. Infante, S.L. Potosf, L. Angeles, Photocatalytic degradation of the herbicide “Paraquat” 39(1999)511–517.
- [30] E. Moctezuma, R. González-garcía, H. Zamarripa, G. Palestino, S. Oros, Kinetic studies of the photocatalytic degradation of the herbicide “Paraquat” 16(2006)343–349.
- [31] K. Tennakone, I.R.M. Kottegoda, Photocatalytic mineralization of paraquat dissolved in water by TiO<sub>2</sub> supported on polythene and polypropylene films. *J. Photochem. Photobiol. A Chem.* 93(1996)79–81.
- [32] A.M. Kouamé, R. Masson, D. Robert, N. Keller, V. Keller,. Beta-SiC foams as a promising structured photocatalytic support for water and air detoxification. *Catal. Today* 209(2013)13–20
- [33] V.Y. Taguchi, S.W.D. Jenkins, P.W. Crozier, , D.T. Wang, . Determination of diquat and paraquat in water by liquid chromatography-(electrospray ionization) mass spectrometry. *J. Am. Soc. Mass Spectrom.* 9(1998)830–839.
- [34] D. Ricketts,. The microbial biodegradation of paraquat in soil. *Pestic. Sci.* 55(1999)596–598.
- [35] T.R. Roberts, D.H. Hutson, P.W. Lee, P.H. Nicholls, J.R. Plimmer, M.C. Roberts, L. Croucher,. *Metabolic Pathways of Agrochemicals: Part 1: Herbicides and Plant Growth Regulators.* Royal Society of Chemistry, 2007.
- [36] J.S. Bus, J.E. Gibson, Paraquat: model for oxidant-initiated toxicity. *Environ. Health Perspect.* 55(1984)37–46.